Atmos. Meas. Tech. Discuss., https://doi.org/10.5194/amt-2019-92
Manuscript under review for journal Atmos. Meas. Tech.
Discussion started: 10 May 2019

Atmospheric Measurement Techniques Discussions

Application of Parametric Speakers to Radio Acoustic Sounding System

Ahoro Adachi[1], Hiroyuki Hashiguchi[2]

[1]Meteorological Research Institute, Tsukuba, 305-0052, Japan
[2]Research Institute for Sustainable Humanosphere, Kyoto University, Uji, 611-0011, Japan

Correspondence to: Ahoro Adachi (aadachi@mri-jma.go.jp)

Abstract. In this study, a wind profiler with radio acoustic sounding system (RASS) and operational radiosonde measurements were used to investigate the technical practicability and reliability of using parametric speakers to measure the vertical profile of virtual temperature. Characteristics of parametric speakers include high directivity and very low sidelobes, which are preferable for RASS, especially those operating at urban areas, if this type of speaker exhibits reliability comparable with acoustic speakers for RASS measurements. The experiments were conducted on fine days with light winds to mitigate the effects of the horizontal and vertical components of wind on acoustic waves used for RASS. The results of this study indicated that, although parametric speaker RASS is susceptible to horizontal winds due to the narrower acoustic beam, bias and standard deviation of parametric speaker RASS/radiosonde virtual temperature difference (0.1°C, 0.4°C) were close to that from acoustic speakers (0.0°C, 0.4°C). In addition, when compared with acoustic speaker RASS, the values for the parametric speaker RASS were even smaller (0.1°C, 0.2°C). Based on these results, it is concluded that the parametric speaker RASS has accuracy and precision comparable with acoustic speaker RASS despite its high directivity of sound.

1 Introduction

Accurate measurements of temperature are essential in weather forecasting and studies of atmospheric dynamics at all scales. The radio acoustic sounding system (RASS) is a ground-based remote sensing technique that provides vertical profiles of virtual temperature from a few hundred meters above the surface up to several kilometers in elevation (Marshall et al., 1972; Peters et al., 1985). RASS technique has been applied to wind profilers, whereby vertical profiles of virtual temperature can be measured with the same temporal and spatial resolution that the profiler uses to measure winds (e.g., Adachi et al., 2005) with a relatively high degree of reliability (Matuura et al., 1986; Moran et al., 1991; Angevine and Ecklund, 1994).

When using RASS techniques, one or more acoustic sources are co-located with an antenna, and the profiler measures the vertical profile of the speed at which the acoustic disturbance propagates vertically (Angevine et al., 1994). RASS temperature measurements can be obtained on the basis of the relationship among the virtual temperature T_v (°C), the local speed of sound C_a (m s^{-1}) and the measured vertical wind speed w (m s^{-1}), and a good approximation can be obtained by

$$T_v = \left(\frac{C_a - w}{20.047}\right)^2 - 273.15. \quad (1)$$

Atmos. Meas. Tech. Discuss., https://doi.org/10.5194/amt-2019-92
Manuscript under review for journal Atmos. Meas. Tech.
Discussion started: 10 May 2019


Atmospheric Measurement Techniques Discussions

Thus, a vertical profile of the speed of sound can be converted to a profile of virtual temperature. The vertical wind speed is considered in Eq. (1) because the neglect of the wind velocity along the beam is the largest source of error in RASS measurements (e.g., May et al., 1989; Angevine et al., 1994).

The bias (systematic error) of the virtual temperature measurements from RASS observations have been shown to be less than 1°C (e.g., Martner et al., 1993; Moran and Strauch, 1994; Angevine and Ecklund, 1994), while the standard deviation (precision) has also been reported around 1°C (Angevine et al., 1998; Martner et al., 1993). In addition, Görsdorf and Lehmann (2000) reported that the bias (standard deviation) of the RASS measurements with a 1.3 GHz wind profiler is 0.1K (0.7K) from the data observed for a year compared with radiosondes if corrections for vertical velocity, range, and constants are applied. On the other hand, the height coverage of RASS depends on the radio wave frequency deployed (May et al., 1988) but is also limited by both the advection of the sound wave with the horizontal wind (Lataitis, 1992) and the atmospheric attenuation of the acoustic signal.

A wind profiler/RASS has been used to study the dynamics of the atmosphere, especially in the boundary layer (e.g., Neiman et al., 1992; Peters and Kirtzel, 1994; May, 1999; Bianco and Wilczak, 2002; White et al., 2003; Adachi et al., 2004; Hashiguchi et al., 2004; Chandrasekhar Sarma et al., 2008). Important limitations of this method include the emission of strong sound waves, whose frequency cannot be arbitrarily selected, but determined by the wavelength of the radio wave used by the profiler to match the Bragg condition (the acoustic wavelength λ_a is equal to half the electromagnetic wavelength λ_e). Although the acoustic speakers used for RASS measurements are usually co-located with the antenna and directed vertically so that the generated sound wave propagates along the radio wave, a large portion of the sound wave leaks horizontally because of the sidelobes of the speakers, which prevents the temporal and/or continuous operation of RASS in urban environments (Wulfmeyer et al., 2015). Thus, a new type of speaker that has extremely low sidelobes is expected for RASS measurements.

A theoretical study of parametric speakers (or parametric acoustic array, PAA) was established by Westervelt (1963). That study revealed that the nonlinear interaction between two collimated high-frequency sound beams in an ideal fluid medium produces two new waves with a sum and difference frequencies, and the latter may be used to produce narrow beams of sound at relatively low audible frequencies. Berktay and Leahy (1974) presented a theoretical description that can be used to compute the far field response of a parametric array for multiple sets of parameters. Hence after, the use of parametric arrays underwater has been the subject of a number of theoretical and experimental studies. On the other hand, an experimental investigation of the parametric array in air was first demonstrated by Bennett and Blackstock (1975), and recently, the parametric loud speaker has become available for audio and speech applications (Gan et al., 2012). The properties of parametric speakers include high directivity and very low sidelobes, which are preferable for RASS measurements. However, to the best of our knowledge, there are few, if any, studies on RASS techniques using this type of speaker.

In this study, a detailed evaluation of the parametric speaker for RASS measurements was conducted by comparing temperature data derived from this type of speaker and those from both radiosonde and acoustic speaker RASS at the

Atmos. Meas. Tech. Discuss., https://doi.org/10.5194/amt-2019-92
Manuscript under review for journal Atmos. Meas. Tech.
Discussion started: 10 May 2019

Meteorological Research Institute (MRI) field site in Tsukuba, Japan. Instrumentation and data analysis techniques are presented in Section 2. Results are presented in Section 3 and discussed in Section 4. Finally, a summary of our conclusions are presented in Section 5.

2 Instrumentation and data analysis techniques

The MRI wind profiler, a four-panel LAP-3000 with RASS (Fig. 1a), is the type originally developed at the National Oceanic Atmospheric Administration (NOAA) Aeronomy Laboratory (Carter et al., 1995; Ecklund et al., 1988). The profiler used in this study operated with 100 m pulse lengths and a minimum (maximum) gate of 200 m (1300 m) from the antenna in RASS mode. The vertical resolution was set to 100 m based on the requirements for the Global Climate Observing System (GCOS) Reference Upper-Air Network (GRUAN) by the WMO (2007). The effect of the vertical air motion was not considered for RASS measurements in the experiments because strong clutter caused by automobiles on a nearby highway sometimes contaminated the Doppler spectrum and masked the atmospheric echo (Adachi et al., 2004). The configuration and operating parameters of the wind profiler/RASS are summarized in Table 1. The antenna of the profiler was co-located with four acoustic speakers in cylindrical enclosures and a parametric speaker, which was mounted on top of a shed (Fig. 1a). In the experiments, the RASS measurements were made continuously for about an hour without wind observations. Since the wind profiler operated at 1.3 GHz, the frequency of the acoustic source for the RASS measurement was set at about 3 kHz to match the Bragg condition. Pseudorandom frequencies (random hop) were chosen for the acoustic source (Angevine et al., 1994) in the experiments.

The MRI parametric speaker, 100FM-001, comprised an array of more than 10,000 piezoelectric ceramic transducers configured on a semi-circular board with a diameter of 1.8 m (Fig. 1b). The transducers were divided into 278 segments, with each one mounted on the hexagonal board (Fig. 1c). The FPGA modules in the speaker system were used to control the phase of the signals fed into the segments to generate the acoustic beam with a particular preferred width and direction like other PAAs (e.g., Wu et al., 2012). The configuration and operating parameters of the speaker are summarized in Table 2.

One of the desirable features of the PAA for RASS measurements is high directivity of the sound beam. Because the beam width of the MRI profiler is less than 7° (Table 1), the default sound beam width of the speaker was designed to be 5° (Table 2). Although the latter width is somewhat smaller than that of the former, the RASS focal spot determined by the sound beam width may be broaden due to turbulence aloft (Lataitis, 1992), which is preferable for the RASS measurements. The audible sound pressure level (SPL) pattern (Fig. 2) measured in the field indicated that the PAA exhibited high directivity and low sidelobes, as expected; the SPL was less than 55 dB at a zenith angle of 40°, which was close to the value of the background noise level of 50 dB despite the fact that the peak power (100 dB) was close to that of an acoustic speaker (105 dB). By contrast, for the acoustic speaker, the SPL was as high as 70 dB even at a zenith (elevation) angle of 85° (5°) and is significantly more annoying to the ear than a PAA.

To evaluate the parametric speaker for RASS measurements, temperature data derived from the PAA-RASS were compared with values derived both from radiosonde and from the acoustic speaker RASS. The dwell time for each RASS measurement was set at about 57 s followed by an intermediate cessation operation time of 3 s, in which the two speaker systems were alternately switched every minute for comparison. Each RASS data set obtained with the two speaker systems was independently processed with quality control to confirm the consistency in the height and time field values.

The profiles of virtual temperature derived from operational radiosonde measurements were used as the standard reference data for comparison. The radiosondes (the Meisei RS-11G used until September 2017, followed by the Meisei iMS-100; Kizu et al., 2018) were launched from the Aerological Observatory, which is located about 400 m northeast of the profiler (for the layout of the relative locations, see Adachi et al., 2004). The time resolution of the radiosonde data used for the comparison was 1 s, which corresponded to the height resolution of about 6 m. The radiosondes were launched operationally at 08:30 JST (Japan Standard Time: JST=UTC+9 h), and most of the RASS experiments included the launch time (Table 3). The RASS data were taken on fine (= no rain) days with light winds (< 3 m s^{-1} on the surface) mostly in autumn when the region was under the influence of a high-pressure system. In the radiosonde comparison, the RASS data were averaged over about an hour for each experiment to mitigate both the effects of vertical velocity (Angevine and Ecklund, 1994; Görsdorf and Lehmann 2000) and the spatial difference between the radiosonde and the profiler/RASS. Contrastingly, the 1 min raw RASS data were used to compare the two speaker systems.

3 Results of comparison

3.1 Availability of parametric speaker for RASS

As there are few, if any, studies on RASS using parametric speakers, preliminary experiments were first conducted to confirm whether the secondary audible waves produced by this type of speaker can propagate long distances along the radio wave while satisfying the Bragg condition before evaluating it for RASS application. The MRI PAA radiates bifrequency primary waves that are around 37 kHz and 40 kHz to generate the parametric sound of the secondary difference frequency, which was around 3 kHz for RASS. Since sound absorption generally increases with frequency, the ultrasound may be substantially dissipated as altitude increases, although the peak SPL of the ultrasonic sound close to the PAA (Table 2) was about 100 dB larger than that of audible sound generated by the acoustic speaker (Fig. 2). The atmospheric absorption is a function of the sound frequency, temperature, humidity, and pressure of the air (ISO, 1993). Example profiles of the sound attenuation coefficient and attenuation at 3 kHz and 40 kHz derived from radiosonde measurements are shown in Fig. 3. In the derivation, only the effect of atmospheric absorption related to viscosity and thermal conductivity of the air, molecular relaxation of rotation, and vibration of O_2 and N_2 was considered (ISO, 1993), and other physical effects (e.g., reflection from the surface; ISO, 1996) were disregarded. Figure 3a shows that the attenuation for the audible wave of 3 kHz propagating from the surface to an altitude of 1 km above ground level (AGL) was 14.7 dB, which indicated that the sound wave at this frequency with an SPL of 105 dB on the ground decreased to 90.3 dB at this altitude. By contrast, this figure

Atmos. Meas. Tech. Discuss., https://doi.org/10.5194/amt-2019-92
Manuscript under review for journal Atmos. Meas. Tech.
Discussion started: 10 May 2019

also suggests that the sound wave at 40 kHz with an SPL of 200 dB generated on the ground was reduced to less than 0 dB at 160 m AGL. Thus, the primary wave of the PAA was not expected to reach beyond this altitude. However, the difference-frequency component could propagate to a higher altitude because it was audible sound.

Figure 4 shows a set of spectra obtained with the acoustic speakers and the PAA at the time when the radiosonde measurement in Fig. 3 was made. The plots were obtained by the LAP-XM, which is a software program developed on the basis of the Profiler On-line Program (POP; Carter et al., 1995). The RASS echoes associated with the acoustic speakers reached as high as 1.3 km AGL. On the other hand, those associated with the PAA also reached a minimum altitude of 1.1 km AGL. Although the PAA-RASS height coverage was somewhat lower than that associated with acoustic speakers, this was much higher than the altitude where the primary ultrasound waves were expected to dissipate. This result suggests that the secondary difference-frequency component can reach the altitude comparable with the audible wave generated by acoustic speakers while satisfying the Bragg condition and propagating along the radio wave as an audible wave.

Another conformity of the secondary audible wave formed by the PAA to the sound wave by the acoustic speaker for the RASS measurement can be seen in the vertical profiles of the received echo power. Samples of the RASS echo power profiles are shown in Fig. 5. The samples were selected from the days (Table 3) when surface winds were light (< 2 m s^{-1}) except on 19 October (Fig. 5a). The RASS echo power of both speaker systems decreased with altitude except for the first range gate. The reason for the decrease may include atmospheric attenuation of the acoustic signal and displacement of the acoustic wave from the radar antenna by the wind (Lataitis, 1992). The echo power with the acoustic speakers was almost always larger than that of the PAA (Figs. 5a–5d). This could be explained by the acoustic speaker's larger peak power than that of the PAA (Fig. 2), and the integrated peak power of the acoustic system, which comprises four speaker units (Fig. 1), could be much larger. The estimation of RASS echo power (e.g. Adachi et al., 1993) was beyond the scope of this study. However, the echo power with both speaker systems in light-wind conditions (Figs. 5b–5d) decreased almost linearly (in dB) with altitude above the first gate, and the difference in the gradient between the two systems was relatively small (less than 15 % on average), although this small difference may also be attributable to the wind. From the facts mentioned above, we concluded that the secondary audible waves formed by the PAA can propagate over a long distance along the radio wave while satisfying the Bragg condition and are applicable to the RASS measurements as the sound wave generated by the acoustic speaker.

Since the PAA was shown to be available for the RASS measurements, we next explored the reliability of the PAA-RASS measurements by comparing with radiosonde observations. It is noteworthy, however, that in Fig. 5a, the echo power with the PAA decreased with altitude more immediately than that associated with the acoustic speaker at altitudes between 300 and 700 m AGL, where relatively high winds were observed, despite the fact that the PAA-RASS echo reached the highest range gate (1300 m AGL) as the acoustic speaker RASS. This suggests that the PAA is more susceptible to high winds than the acoustic speakers. Thus, the effect of wind on the PAA-RASS measurements is discussed later in this paper.

Atmos. Meas. Tech. Discuss., https://doi.org/10.5194/amt-2019-92
Manuscript under review for journal Atmos. Meas. Tech.
Discussion started: 10 May 2019


Atmospheric Measurement Techniques Discussions

3.2 Comparisons with radiosonde

Profiles of virtual temperature (*Tv*) derived from radiosonde, the PAA-RASS, and the acoustic speaker RASS observations are shown in Fig. 6 along with the corresponding statistics for the data. The *Tv* derived from the radiosondes was in good agreement with the RASS measurements derived from both speaker systems, lying within the error bar of most of the range gates. In addition, *Tv* derived with both speaker systems were close to each other. However, bias and standard deviation tended to be large at inversion layers and at the first gate (e.g., Figs. 6b and 6c), the latter of which may corresponded to the smaller received power at that gate as shown in Fig. 5. This could be attributable to the fact that the first gate is too close to the antenna and need to apply a range correction to obtain reliable data (e.g., Görsdorf and Lehmann, 2000; Johnston et al., 2002).

Scatter diagrams comparing radiosonde virtual temperature with that from RASS for all experiments are shown in Fig. 7 along with statistics. The RASS data were averaged for about an hour. The radiosonde data were smoothed by 100 m running means to match the RASS observations. The first range gate data of the RASS measurements were not considered because they are less reliable. This figure shows that both the PAA and acoustic speaker RASS measurements of virtual temperature were generally in good agreement with those derived from radiosonde measurements, as expected. The linear regressions for both speaker systems were close to the one-to-one relation, and correlation coefficients were close to unity. In addition, the systematic error was less than 0.1 °C and the standard deviation was 0.4°C for both systems, suggesting that both systems are reliable for RASS measurements.

4 Discussions

As reported above, we found many instances in which the PAA speaker system exhibited comparable performance with the acoustic speakers with respect to the RASS measurements in observing profiles of the Doppler spectrum and the virtual temperature, as shown in the statistics for the comparisons both with radiosonde and with the acoustic speaker RASS. Indeed, the bias and standard deviation for each speaker system RASS with respect to radiosonde were in good agreement with results reported in previous studies (e.g., Görsdorf and Lehmann 2000), despite no correction for vertical velocity, which could have been partly because of the experiments being conducted on fine days with light wind and the application of a relatively long averaging time. In addition, removing the first gate data from the statistics may also contribute to the results.

Although applying a long averaging time could mitigate the effect of vertical airflow on bias (e.g., Moran and Strauch, 1994), it may degrade the statistics when the virtual temperature profile evolves within the duration of the RASS measurement. On the other hand, the statistics also indicated that the data number associated with the PAA was smaller than that of the acoustic speakers (e.g., Fig. 6), implying that the mean height coverage with the former was lower than that of the latter presumably because of wind in addition to the low peak power mentioned previously. Thus, we independently focus

Atmos. Meas. Tech. Discuss., https://doi.org/10.5194/amt-2019-92
Manuscript under review for journal Atmos. Meas. Tech.
Discussion started: 10 May 2019


Atmospheric Measurement Techniques Discussions

our attention on both the effects of the time evolution of the temperature profile on the statistics and of wind on the height coverage of the RASS measurement in the following sections.

4.1 Effect of rapid time evolution of temperature profile

In the comparisons, the RASS data were averaged for a relatively long time to minimize the effects of both vertical velocity and the spatial difference between the radiosonde and the profiler/RASS. However, the temperature profiles derived from radiosonde observations may not be well suited for use as standard reference data if the temperature profile evolved rapidly within the hour-long RASS observation duration. In the experiments, since the operational radiosondes were launched in the morning of fine days, an inversion layer was frequently observed (Fig. 6). In fact, 12 inversions including multiple inversion layers (e.g., Fig. 6b) were observed in 8 of the 16 experiments. Inversion layers can evolve in a relatively short time due to surface heating and cooling and/or the development of the boundary layer in the morning. Indeed, the surface virtual temperature increased by 2.3°C on average within an hour for the experiments shown in Fig. 6. In this case, the temperature profile measured with the radiosonde can differ from the mean temperature profile obtained from RASS even though both measurements represented an actual profile, which may result in degrading the statistics for the RASS evaluation.

A sample of the temperature profile observing an inversion layer is shown in Fig. 8. The *Tv* profiles with error bars were the mean RASS measurements averaged over an hour from acoustic (red) and PAA (blue) speakers. Both RASS profiles represented the radiosonde profile to some extent but did not follow the profile well, especially around the inversion layer. The large standard deviations indicated by long error bars may reflect the time evolution of the temperature profile in addition to the measurement precision of RASS. By contrast, the 1 min raw RASS data recorded around the radiosonde launch time represented the inversion layer better than the mean RASS measurements, although there were still some discrepancies, which may have been due to the locality of the inversion layer, the effect of vertical air motion, or the time difference between RASS and radiosonde in addition to the accuracy and precision of the RASS measurements. In terms of the time difference, it is noteworthy that the radiosonde measurement is not a snapshot but sequential; it took more than 2 min for the radiosonde to ascend to an altitude of 800 m AGL, and the temperature profile may evolve even during this time. Thus, a comparison with measurements that have both small spatial difference and high time resolution is needed to evaluate the PAA-RASS measurement.

4.2 Comparison with acoustic speaker RASS

To suppress the effects of the spatial and time difference between the two platforms on the evaluation, we next compared the temperatures derived from the PAA-RASS with that from the acoustic speaker RASS. Of course, this comparison does not provide an absolute but relative evaluation of the PAA-RASS measurement. This issue should be kept in mind in examining the intercomparisons presented in this section. In the intercomparison, the requirements for high-quality upper-air reference data (bias $\leq$ 0.1K , $\sigma \leq$ 0.2K) proposed by WMO (2007) for the GRUAN were used as criteria for the evaluation, although they are not for virtual temperature but for real temperature.

Atmos. Meas. Tech. Discuss., https://doi.org/10.5194/amt-2019-92
Manuscript under review for journal Atmos. Meas. Tech.
Discussion started: 10 May 2019


Atmospheric Measurement Techniques Discussions

A normalized frequency diagram and scatterplot of virtual temperature obtained by the acoustic speaker RASS versus the PAA-RASS are shown in Fig. 9. The 1 min raw data obtained alternately are presented in Fig. 9a, whereas the data averaged for about an hour are plotted in Fig. 9b. Figure 9a shows that the PAA-RASS measurements of virtual temperature were generally in good agreement with those of the acoustic speaker RASS despite disregarding the time difference in the two systems. The linear regression line was close to the one-to-one relation, and the correlation coefficient was close to unity. Moreover, the mean bias and standard deviation of the difference between the two speaker systems were less than 0.1°C and close to 0.4°C, respectively, which are comparable with those obtained by the comparison with radiosonde (Fig. 7) despite the higher time resolution. Since the spatial difference was negligible, the reason for this discrepancy could include the effect of the time difference on temperature associated with atmospheric phenomena, such as the development of the boundary layer by surface heating and cooling, and/or advection of a warm/cold air mass. Indeed, the mean (max and min) increase of the virtual temperature at the surface for all the experiments was 0.2±0.5°C/10 min (1.4°C/10 min, –1.3°C/10 min), which suggests that temperature fluctuation aloft was occurring.

A scatter diagram comparing the mean acoustic speaker RASS measurements with those from the parametric speaker RASS is shown in Fig. 9b. The data were averaged over about an hour to minimize the effect of temporal fluctuation of temperature and improve the statistics. Indeed, the linear regression was close to the one-to-one relation, and the correlation coefficient was closer to unity. In addition, both the bias (0.06°C) and standard deviation (0.16°C) improved and satisfied the WMO requirements.

From the evaluations mentioned above, we conclude that the accuracy and precision of the parametric speaker RASS are comparable with those of the acoustic speaker RASS for measuring the vertical profile of virtual temperature. The reliability of the parametric speaker RASS could be improved by applying the time average over the appropriate period, advanced quality control, and/or corrections for both range and vertical airflow as long as the effect of the ground clutter is negligibly small.

4.3 Effect of horizontal wind on the height coverage of the RASS measurement

The reliability of the parametric speaker RASS measurement was shown to be equivalent to the acoustic speaker RASS. However, we found many instances in which the former tended to have less height coverage than the latter (Figs. 4, 5, and 6), which is also reflected by the fewer number of data in the statistics (Figs. 6, 7, and 8). Although the parametric speaker system exhibited less peak power than the acoustic speaker system, the weak power cannot be the only reason for the lower height coverage because the results show that the former can observe up to the highest range gate as the latter in some conditions (e.g., Figs. 5a, 5b, 6a, and 8). On the other hand, the results also suggest that the reason may include the effect of wind aloft (e.g., Fig. 5a). Because the acoustic beam generated by the parametric speaker is narrow, it could be susceptible to the horizontal airflow, which displaces the acoustic wave from the radar antenna. Thus, the effect of horizontal wind on the height coverage of the parametric speaker RASS measurement was evaluated by comparing it with the radiosonde wind data.

Atmos. Meas. Tech. Discuss., https://doi.org/10.5194/amt-2019-92
Manuscript under review for journal Atmos. Meas. Tech.
Discussion started: 10 May 2019

Atmospheric Measurement Techniques Discussions

A scatter diagram comparing the mean RASS height coverage and radiosonde wind speed aloft (Table 3) is shown in Fig. 10. The wind speed aloft is the mean wind from 1 to 1200 m AGL, which is the highest mean coverage of the parametric speaker RASS measurements in calm wind conditions (< 2 m s^{-1}) as shown in the figure. The data measured on 30 November 2016 are not considered in the analysis because the RASS measurement was made more than 40 min later than the radiosonde observation (Table 3). The parametric speaker RASS measurements tended to reach less altitude than acoustic speaker RASS even in light-wind conditions (< 3 m s^{-1}). The reason for less coverage in light-wind conditions may be due to the parametric speaker's lower peak power than the acoustic speaker system. The height coverage decreased with wind speed for both speaker systems as indicated by the linear regression analysis. However, the individual data indicated that when the mean wind speed was less than 6 m s^{-1}, most of the acoustic speaker RASS measurements achieved a height coverage of around 1300 m AGL, which was the highest range gate for the RASS measurement (Table 1). This suggests that the acoustic speaker RASS could observe higher altitude in relatively high wind conditions.

It is noteworthy, however, that the height coverage of RASS with acoustic speakers drops sharply to 1000 m AGL at a wind speed of around 5–6 m s^{-1}, and exhibits a tendency to decrease with wind afterward as the parametric speaker RASS. By contrast, the height coverage of the parametric speaker tends to decrease monotonically with wind at all ranges. These results suggest that the parametric speaker RASS is more sensitive to wind because of the narrow beam, whereas the acoustic speaker RASS is surprisingly robust. Since the four acoustic speakers were not adjusted in phase, this robustness could be explained by the integrated beam width, which could be larger than that shown in Fig. 2, and the sound wave locates above the antenna even in relatively high wind conditions.

To compensate for the lower wind tolerance, two additional experiments were performed, in which the acoustic beam was broadened and steered. The parametric speaker system employed for the RASS experiments was equipped with FPGA that controlled the beam pattern of the sound, including beam width and direction. We broadened the beam width from 5° to 12° (Fig. 2) when the parametric RASS echo was observed up to an altitude of 1200 m AGL. However, this experiment resulted in a decrease of the height coverage to 500 m AGL. The height coverage decrease could have been due to the decrease of the peak power associated with beam broadening. In fact, the measured peak power was decreased by 15 dB in our system by broadening the beam (Fig. 2). Therefore, by using this technique, a parametric speaker with more peak power was needed in our case to acquire equivalent height coverage with the acoustic speaker system, which may result in increasing both the size and cost of the system.

On the other hand, the peak power does not decrease significantly with the zenith angle of the beam as long as the angle is small. The results indicated that the peak power decreased by only 3.8 dB when the beam was steered to a zenith angle of 10° (Fig. 11), which corresponds to a horizontal wind speed of 60 m s^{-1}. The sound wave might be displaced by the horizontal wind but advected to above the antenna if the wave is generated windward with an appropriate zenith angle. Thus, we conducted another experiment with the acoustic beam zenith angle of 2° windward on a day when a mean wind speed of about 12 m s^{-1} between 200 and 1200 m AGL was observed with the wind profiler. Unfortunately, no RASS echo was observed, which may be partly because the sound wave did not propagate vertically to the ground, and the advected sound

wave front above the antenna was not normal to the propagation direction of the radio wave. Additionally, the acoustic wave front may be distorted by wind shear. In that case, the radio wave may be needed to be steered to the direction normal to the sound wave front by considering the advection and distortion of the sound wave front from the wind profiler measurements.

5 Conclusions

We investigated the availability of parametric speakers for RASS for measuring the vertical profile of virtual temperature by comparing the data with those obtained from both radiosonde and the acoustic speaker RASS. In the experiments, the operations of the two speaker systems were swapped every minute alternately for the comparison. A detailed analysis of the profiles of both the acoustic attenuation and the Doppler spectrum suggest that although the primary ultrasound generated by the parametric speaker may be dissipated greatly as altitude increases, the secondary audible waves generated from the bifrequency ultrasound can propagate long distances while satisfying the Bragg condition.

We have also compared parametric speakers with both radiosonde and acoustic speakers to estimate the reliability of RASS in measuring the virtual temperature. The results indicated that *Tv* measured with parametric speaker RASS has comparable reliability with the acoustic speaker RASS measurements; the bias and standard deviation (0.1°C, 0.4°C) for the parametric speaker were close to those for the acoustic speaker (0.0°C, 0.4°C) with respect to radiosonde, which was consistent with results reported in previous studies. We also found that not only the spatial difference between the two platforms but also the evolution of the temperature profile during the RASS measurement could contribute to deteriorate the statistics. To mitigate the effects of both the spatial differences and temperature evolution with time, a comparison of virtual temperature obtained from the two speaker systems was also performed. The results indicated that the bias and standard deviation (0.1°C, 0.2°C) of the parametric speaker RASS were quite small and satisfied the requirements for high-quality upper-air reference data proposed by the WMO (2007). Taken together, we conclude that parametric speaker RASS has comparable accuracy and precision with acoustic speaker RASS with respect to the measurement of the virtual temperature profile.

We examined the height coverage of RASS and found that the parametric speaker deployed in the experiments tended to have less coverage than does the acoustic speakers, which may be a result of the parametric speaker having high directivity, and the generated sound was more susceptible to the displacement from the radar antenna by horizontal wind than the sound wave by the acoustic speakers. Thus, we broadened the beam width of the parametric speaker, which resulted in degrading height coverage because this operation deteriorates the peak power of the audible sound. The sound wave was then steered windward so that the advected sound was located above the antenna. However, no echo was observed, presumably because the sound wave front advected to above the antenna was not normal to the propagation direction of the radio wave in the experiments. In addition, the sound wave front may have been distorted by wind shear. This issue might be solved by using wind profilers that are capable of steering the radio wave (e.g., Adachi and Kobayashi, 2001; Law et al., 2002; Palmer et al., 2005) to the direction normal to the sound wave front as Masuda (1988) proved with the MU radar (Fukao et al., 1985).

The results of this study including the statistics do not necessarily apply to all locations, altitudes, and seasons; in particular, we note that the comparisons in this case study were made in the morning on fine days with light wind when the effects of horizontal and vertical wind would be less expected. This condition is possible even in other seasons, but frequency is likely to be less.

In summary, we confirm that a parametric speaker is applicable to RASS measurement with a reliability comparable with acoustic speakers. Although it is sensitive to horizontal wind, this type of speaker could be installed to wind profilers located in urban areas for continuous-operational observations (e.g., Ishihara et al., 2006) to improve weather forecast because it has high directivity and no horizontal sound wave leaks to annoy nearby residents.

Acknowledgements

The authors wish to thank Emeritus Professor T. Tsuda of Kyoto University for many helpful discussions and comments regarding the research presented and Mr. S. Hoshino of the Aerological Observatory for providing information on radiosonde measurements. The first author wishes to thank Mr. J. Neuschaefer of Vaisala for offering the LAP-XM software to analyze the spectrum data, Mr. S. Onogi of the Meteorological Instrument Centre, Mr. N. Okushima of Starlite Co., Ltd. and Mr. T. Takai for technical support, and Drs. Y. Shoji, M. Mikami, A. Segami, and S. Tsunomura of MRI, JMA for providing an opportunity to conduct the experiments. This study was partially supported by JSPS KAKENHI Grant Number 15K01273 and 17H00852.

References

Adachi, A., Clark, W. L., Hartten, L. M., Gage, K. S., and Kobayashi, T.: An observational study of a shallow gravity current triggered by katabatic flow, Ann. Geophys., 22, 3937-3950, doi: 10.5194/angeo-22-3937-2004, 2004.

Adachi, A. and Kobayashi, T.: RHI observations of precipitation with boundary wind profiler, Munich, 2001, 116-117.

Adachi, A., Kobayashi, T., Gage, K. S., Carter, D. A., Hartten, L. M., Clark, W. L., and Fukuda, M.: Evaluation of three-beam and four-beam profiler wind measurement techniques using a five-beam wind profiler and collocated meteorological tower, J. Atmos. Oceanic Technol., 22, 1167-1180, doi: 10.1175/jtech1777.1, 2005.

Adachi, T., Tsuda, T., Masuda, Y., Takami, T., Kato, S., and Fukao, S.: Effects of the acoustic and radar pulse length ratio on the accuracy of radio acoustic sounding system (RASS) temperature measurements with monochromatic acoustic pulses, Radio Sci., 28, 571-583, doi: 10.1029/93RS00359, 1993.

Angevine, W. M., Bakwin, P. S., and Davis, K. J.: Wind profiler and RASS measurements compared with measurements from a 450-m-tall tower, J. Atmos. Oceanic Technol., 15, 818-825, doi: 10.1175/1520-0426(1998)015<0818:Wparmc>2.0.Co;2, 1998.

Angevine, W. M. and Ecklund, W. L.: Errors in radio acoustic sounding of temperature, J. Atmos. Oceanic Technol., 11, 837-842, doi: 10.1175/1520-0426(1994)011<0837:EIRASO>2.0.CO;2, 1994.

Angevine, W. M., Ecklund, W. L., Carter, D. A., Gage, K. S., and Moran, K. P.: Improved radio acoustic sounding techniques, J. Atmos. Oceanic Technol., 11, 42-49, doi: 10.1175/1520-0426(1994)011<0042:IRAST>2.0.CO;2, 1994.

Bennett, M. B. and Blackstock, D. T.: Parametric array in air, J. Acoust. Soc. Am., 57, 562-568, doi: 10.1121/1.380484, 1975.

Berktay, H. O. and Leahy, D. J.: Farfield performance of parametric transmitters, J. Acoust. Soc. Am., 55, 539-546, doi: 10.1121/1.1914533, 1974.

Bianco, L. and Wilczak, J. M.: Convective boundary layer depth: Improved measurement by Doppler radar wind profiler using fuzzy logic methods, J. Atmos. Oceanic Technol., 19, 1745-1758, doi: 10.1175/1520-0426(2002)019<1745:CBLDIM>2.0.CO;2, 2002.

Carter, D. A., Gage, K. S., Ecklund, W. L., Angevine, W. M., Johnston, P. E., Riddle, A. C., Wilson, J., and Williams, C. R.: Developments in UHF lower tropospheric wind profiling at NOAA's Aeronomy Laboratory, Radio Sci., 30, 977-1001, doi: 10.1029/95RS00649, 1995.

Chandrasekhar Sarma, T. V., Narayana Rao, D., Furumoto, J., and Tsuda, T.: Development of radio acoustic sounding system (RASS) with Gadanki MST radar – first results, Ann. Geophys., 26, 2531-2542, doi: 10.5194/angeo-26-2531-2008, 2008.

Ecklund, W. L., Carter, D. A., and Balsley, B. B.: A UHF wind profiler for the boundary layer: Brief description and initial results, J. Atmos. Oceanic Technol., 5, 432-441, doi: 10.1175/1520-0426(1988)005<0432:AUWPFT>2.0.CO;2, 1988.

Fukao, S., Sato, T., Tsuda, T., Kato, S., Wakasugi, K., and Makihira, T.: The MU radar with an active phased array system: 1. Antenna and power amplifiers, Radio Sci., 20, 1155-1168, doi: 10.1029/RS020i006p01155, 1985.

Gan, W.-S., Yang, J., and Kamakura, T.: A review of parametric acoustic array in air, Appl. Acoust., 73, 1211-1219, doi: 10.1016/j.apacoust.2012.04.001, 2012.

Görsdorf, U. and Lehmann, V.: Enhanced accuracy of RASS-measured temperatures due to an improved range correction, J. Atmos. Oceanic Technol., 17, 406-416, doi: 10.1175/1520-0426(2000)017<0406:Eaormt>2.0.Co;2, 2000.

Hashiguchi, H., Fukao, S., Moritani, Y., Wakayama, T., and Watanabe, S.: A lower troposphere radar: 1.3-GHz active phased-array type wind profiler with RASS, J. Meteor. Soc. Japan, 82, 915-931, doi: 10.2151/jmsj.2004.915, 2004.

Ishihara, M., Kato, Y., Abo, T., Kobayashi, K., and Izumikawa, Y.: Characteristics and performance of the operational wind profiler network of the Japan Meteorological Agency, J. Meteor. Soc. Japan, 84, 1085-1096, doi: 10.2151/jmsj.84.1085, 2006.

ISO: 9613-1, Acoustics - Attenuation of sound during propagation outdoors - Part 1: Calculation of the absorption of sound by the atmosphere, 1993. 30pp, 1993.

ISO: 9613-2, Acoustics - Attenuation of sound during propagation outdoors - Part 2: General method of calculation, 1996. 18pp, 1996.

Johnston, P. E., Hartten, L. M., Love, C. H., Carter, D. A., and Gage, K. S.: Range errors in wind profiling caused by strong reflectivity gradients, J. Atmos. Oceanic Technol., 19, 934-953, doi: 10.1175/1520-0426(2002)019<0934:REIWPC>2.0.CO;2, 2002.

Kizu, N., Sugidachi, T., Kobayashi, E., Hoshino, S., Shimizu, K., Maeda, R., and Fujiwara, M.: Technical characteristics and GRUAN data processing for the Meisei RS-11G and iMS-100 radiosondes, GRUAN-TD-5, GRUAN Lead Centre, 2018.

Lataitis, R. J.: Signal power for radio acoustic sounding of temperature: The effects of horizontal winds, turbulence, and vertical temperature gradients, Radio Sci., 27, 369-385, doi: doi:10.1029/92RS00004, 1992.

Law, D. C., McLaughlin, S. A., Post, M. J., Weber, B. L., Welsh, D. C., Wolfe, D. E., and Merritt, D. A.: An electronically stabilized phased array system for shipborne atmospheric wind profiling, J. Atmos. Oceanic Technol., 19, 924-933, doi: 10.1175/1520-0426(2002)019<0924:AESPAS>2.0.CO;2, 2002.

Marshall, J. M., Peterson, A. M., and Barnes, A. A.: Combined Radar-Acoustic Sounding System, Applied Optics, 11, 108-112, doi: 10.1364/AO.11.000108, 1972.

Martner, B. E., Wuertz, D. B., Stankov, B. B., Strauch, R. G., Westwater, E. R., Gage, K. S., Ecklund, W. L., Martin, C. L., and Dabberdt, W. F.: An evaluation of wind profiler, RASS, and microwave radiometer performance, Bull. Amer. Meteor. Soc., 74, 599-614, doi: 10.1175/1520-0477(1993)074<0599:AEOWPR>2.0.CO;2, 1993.

Masuda, Y.: Influence of wind and temperature on the height limit of a radio acoustic sounding system, Radio Sci., 23, 647-654, doi: 10.1029/RS023i004p00647, 1988.

Matuura, N., Masuda, Y., Inuki, H., Kato, S., Fukao, S., Sato, T., and Tsuda, T.: Radio acoustic measurement of temperature profile in the troposphere and stratosphere, Nature, 323, 426, doi: 10.1038/323426a0, 1986.

May, P. T.: Thermodynamic and vertical velocity structure of two gust fronts observed with a wind profiler/RASS during MCTEX, Mon. Wea. Rev., 127, 1796-1807, doi: 10.1175/1520-0493(1999)127<1796:TAVVSO>2.0.CO;2, 1999.

May, P. T., Moran, K. P., and Strauch, R. G.: The accuracy of RASS temperature measurements, J. Appl. Meteor, 28, 1329-1335, doi: 10.1175/1520-0450(1989)028<1329:Taortm>2.0.Co;2, 1989.

May, P. T., Strauch, R. G., and Moran, K. P.: The altitude coverage of temperature measurements using RASS with wind profiler radars, Geophys. Res. Lett., 15, 1381-1384, doi: 10.1029/GL015i012p01381, 1988.

Moran, K. P. and Strauch, R. G.: The accuracy of RASS temperature measurements corrected for vertical air motion, J. Atmos. Oceanic Technol., 11, 995-1001, doi: 10.1175/1520-0426(1994)011<0995:TAORTM>2.0.CO;2, 1994.

Moran, K. P., Wuertz, D. B., Strauch, R. G., Abshire, N. L., and Law, D. C.: Temperature sounding with wind profiler radars, J. Atmos. Oceanic Technol., 8, 606-608, doi: 10.1175/1520-0426(1991)008<0606:Tswwpr>2.0.Co;2, 1991.

Neiman, P. J., May, P. T., and Shapiro, M. A.: Radio acoustic sounding system (RASS) and wind profiler observations of lower- and midtropospheric weather systems, Mon. Wea. Rev., 120, 2298-2313, doi: 10.1175/1520-0493(1992)120<2298:RASSAW>2.0.CO;2, 1992.

Palmer, R. D., Cheong, B. L., Hoffman, M. W., Frasier, S. J., and López-Dekker, F. J.: Observations of the small-scale variability of precipitation using an imaging radar, J. Atmos. Oceanic Technol., 22, 1122-1137, doi: 10.1175/JTECH1775.1, 2005.

Peters, G., Hinzpeter, H., and Baumann, G.: Measurements of heat flux in the atmospheric boundary layer by sodar and RASS: A first attempt, Radio Sci., 20, 1555-1564, doi: 10.1029/RS020i006p01555, 1985.

Peters, G. and Kirtzel, H. J.: Measurements of Momentum Flux in the Boundary Layer by RASS, J. Atmos. Oceanic Technol., 11, 63-75, doi: 10.1175/1520-0426(1994)011<0063:Momfit>2.0.Co;2, 1994.

Westervelt, P. J.: Parametric Acoustic Array, J. Acoust. Soc. Am., 35, 535-537, doi: 10.1121/1.1918525, 1963.

White, A. B., Neiman, P. J., Ralph, F. M., Kingsmill, D. E., and Persson, P. O. G.: Coastal orographic rainfall processes observed by radar during the California Land-Falling Jets Experiment, J. Hydrometeor., 4, 264-282, doi: 10.1175/1525-7541(2003)4<264:CORPOB>2.0.CO;2, 2003.

WMO: GCOS Reference Upper-Air Network (GRUAN): Justification, requirements, siting and instrumentation options, GCOS-112, WMO/TD 1379, 2007.

Wu, S., Wu, M., Huang, C., and Yang, J.: FPGA-based implementation of steerable parametric loudspeaker using fractional delay filter, Appl. Acoust., 73, 1271-1281, doi: 10.1016/j.apacoust.2012.04.013, 2012.

Wulfmeyer, V., Hardesty, R. M., Turner, D. D., Behrendt, A., Cadeddu, M. P., Di Girolamo, P., Schlüssel, P., Van Baelen, J., and Zus, F.: A review of the remote sensing of lower tropospheric thermodynamic profiles and its indispensable role for the understanding and the simulation of water and energy cycles, Rev. Geophys., 53, 819-895, doi: 10.1002/2014RG000476, 2015.

Atmos. Meas. Tech. Discuss., https://doi.org/10.5194/amt-2019-92
Manuscript under review for journal Atmos. Meas. Tech.
Discussion started: 10 May 2019

Atmospheric Measurement Techniques Discussions

Table 1. Parameters of the wind profiler/RASS.

Frequency	1357.5 MHz
Peak Power	500 W
Beam width	< 7°
Beam elevation	90°
Pulse width	665 ns
First range gate	200 m
Last range gate	1300 m
Gate spacing	100 m
Interpulse period	12163 ns
Coherent Integration	3
Spectra Averaged	191
Number of FFT points	8192
Manufacture	Scintec
Model	LAP-3000

Atmos. Meas. Tech. Discuss., https://doi.org/10.5194/amt-2019-92
Manuscript under review for journal Atmos. Meas. Tech.
Discussion started: 10 May 2019

Atmospheric Measurement Techniques Discussions

Table 2. Characteristics of the MRI parametric speaker.

Center frequency	40.0±1.0 kHz
Band width (-6dB)	< 2.0 kHz
Sound pressure level	> 200 dB (at 0.3m, 40 kHz, theoretical value)
Number of transducers	10008
Number of channels	278
Beam width	5°—17° (1° step)
Beam elevation	60—90° (1° step)
Beam azimuth	0—359° (1° step)
Input audio signal freq.	2.8—3.3 kHz
Modulation	AM (DSB)
Speaker diameter	1.8 m
Speaker system size	2.1 x 2.1 x 1.8 m
Manufacture	Starlite Co., Ltd.
Model	100FM-001

Atmos. Meas. Tech. Discuss., https://doi.org/10.5194/amt-2019-92
Manuscript under review for journal Atmos. Meas. Tech.
Discussion started: 10 May 2019

Atmospheric Measurement Techniques Discussions

Table 3. List of the comparison experiments, including date, period, sea level pressure, surface temperature, surface wind speed, and mean wind speed aloft.

Date	Time [JST]	P_{sea} [hPa]	T [°C]	W [m s^{-1}]	$\overline{W}_{aloft}$ [m s^{-1}]
14 Oct. 2016	0803–0900	1023.0	15.0	2.0	5.8±2.8
15 Oct. 2016	0801–0900	1025.5	15.8	1.4	2.1±0.5
19 Oct. 2016	0801–0900	1015.6	20.2	3.1	5.4±1.7
21 Oct. 2016	0801–0900	1016.5	15.7	2.1	3.1±0.7
24 Oct. 2016	0819–0900	1014.9	13.1	2.0	3.2±1.5
27 Oct. 2016	0837–0932	1016.1	18.8	0.8	1.6±0.6
28 Oct. 2016	0803–0900	1018.4	12.5	1.2	7.6±3.3
31 Oct. 2016	0809–0900	1024.3	12.7	1.7	5.4±2.6
02 Nov. 2016	0825–0902	1023.2	9.8	1.6	5.0±2.3
08 Nov. 2016	0803–0902	1017.0	7.4	2.2	5.4±3.4
12 Nov. 2016	0809–0906	1019.8	11.8	0.4	3.7±1.3
30 Nov. 2016	0911–0932	1030.4	5.7	1.8	2.9±1.4
29 Mar. 2017	0843–0900	1020.0	8.4	2.4	4.9±1.3
09 Aug. 2017	0845–0900	991.3	30.5	1.2	4.5±2.5
07 Sep. 2017	0801–0900	1003.2	22.3	1.8	2.3±0.5
09 Apr. 2018	0825–0902	1013.6	10.2	1.6	6.9±5.1

Atmos. Meas. Tech. Discuss., https://doi.org/10.5194/amt-2019-92
Manuscript under review for journal Atmos. Meas. Tech.
Discussion started: 10 May 2019

Atmospheric Measurement Techniques Discussions

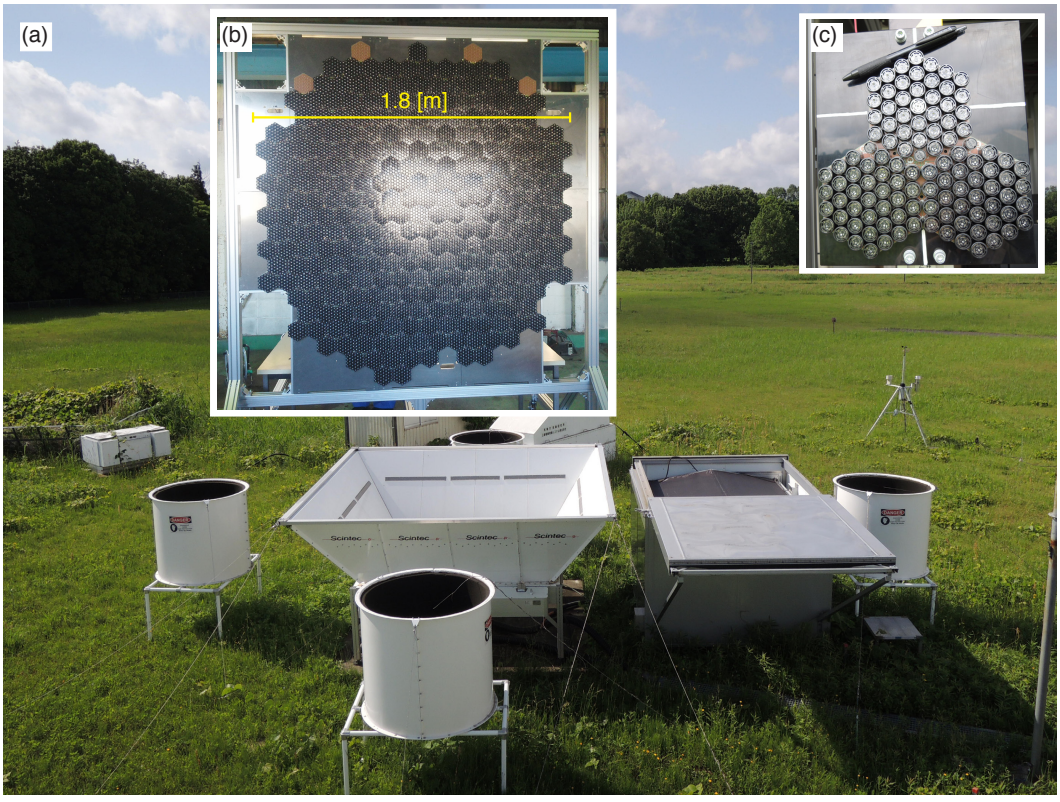

Figure 1. Pictures of (a) LAP-3000 with acoustic speakers and a parametric speaker for RASS, (b) top view, and (c) partial expanded view of the parametric speaker. The parametric speaker mounted on top of the shed with a sliding roof is covered with rainproof film in the field, as shown in (a).

Atmos. Meas. Tech. Discuss., https://doi.org/10.5194/amt-2019-92
Manuscript under review for journal Atmos. Meas. Tech.
Discussion started: 10 May 2019

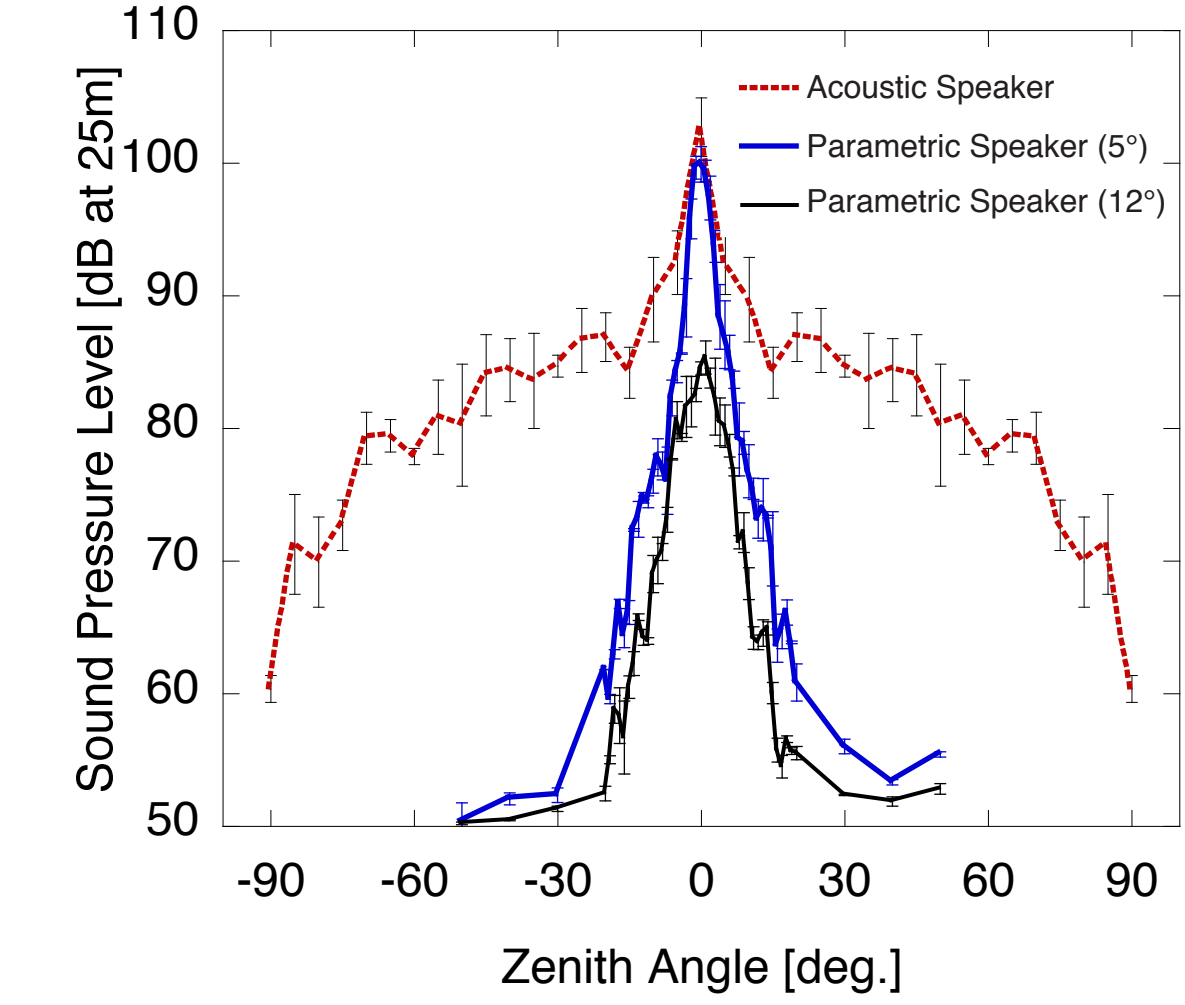

Figure 2. Audible sound pressure level (SPL) pattern for an acoustic speaker (red), the parametric speaker with the measured beam width of 5° (blue) and 12° (black) at a frequency of 3 kHz. The error bars represent 2σ. The SPL pattern for the acoustic speaker in the negative zenith angle region is a mirror image of the pattern measured at the positive zenith angle for ease of viewing. The background noise level was about 50 dB. The SPL was measured with a sound level meter (Rion NL-42).

Atmos. Meas. Tech. Discuss., https://doi.org/10.5194/amt-2019-92
Manuscript under review for journal Atmos. Meas. Tech.
Discussion started: 10 May 2019

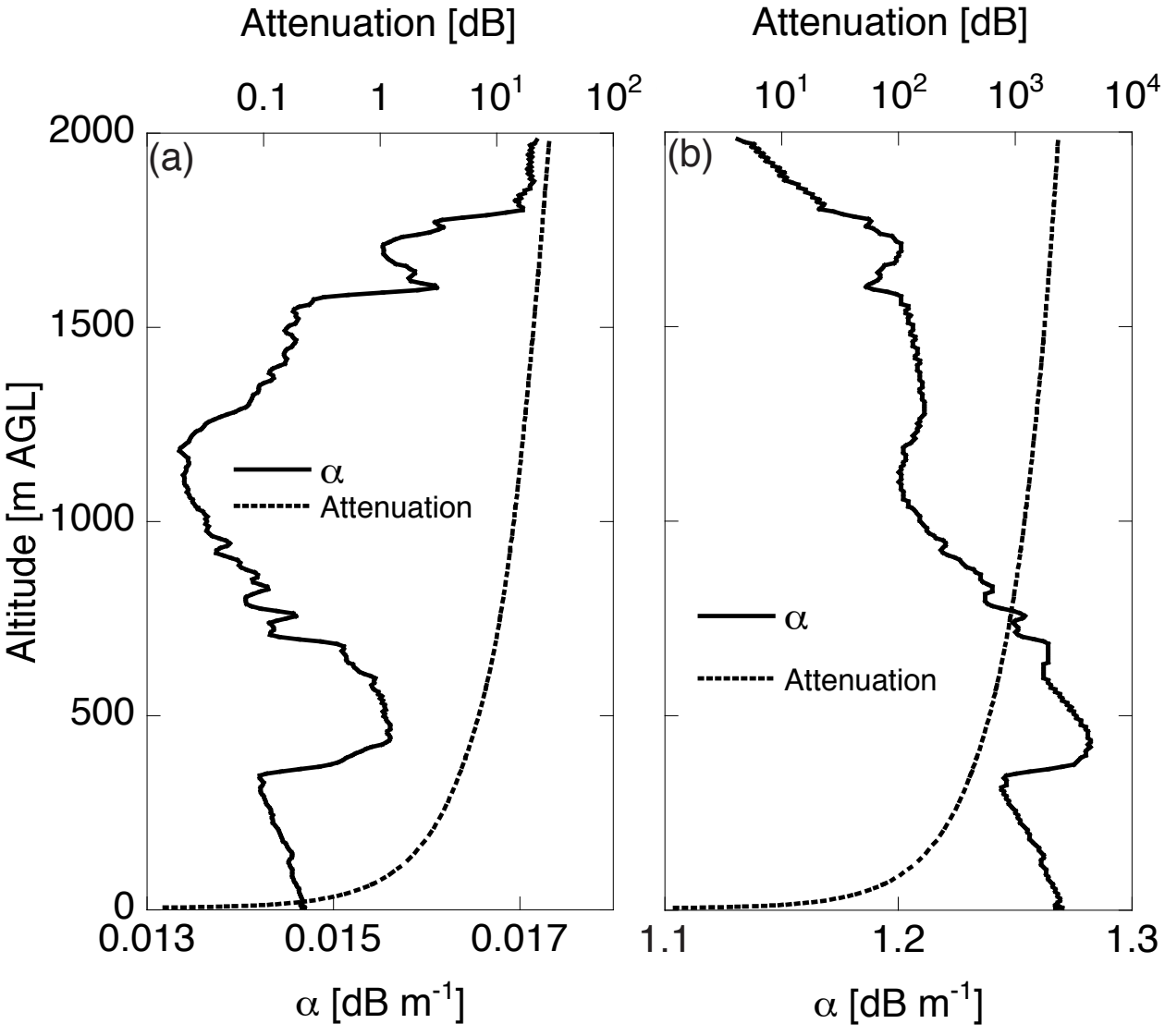

Figure 3. Profiles of atmospheric-attenuation coefficient α and atmospheric attenuation for sound at frequencies of (a) 3 kHz and (b) 40 kHz derived from the radiosonde measurements at 08:30 JST on 19 October 2016, at the MRI site.

5

Atmos. Meas. Tech. Discuss., https://doi.org/10.5194/amt-2019-92
Manuscript under review for journal Atmos. Meas. Tech.
Discussion started: 10 May 2019

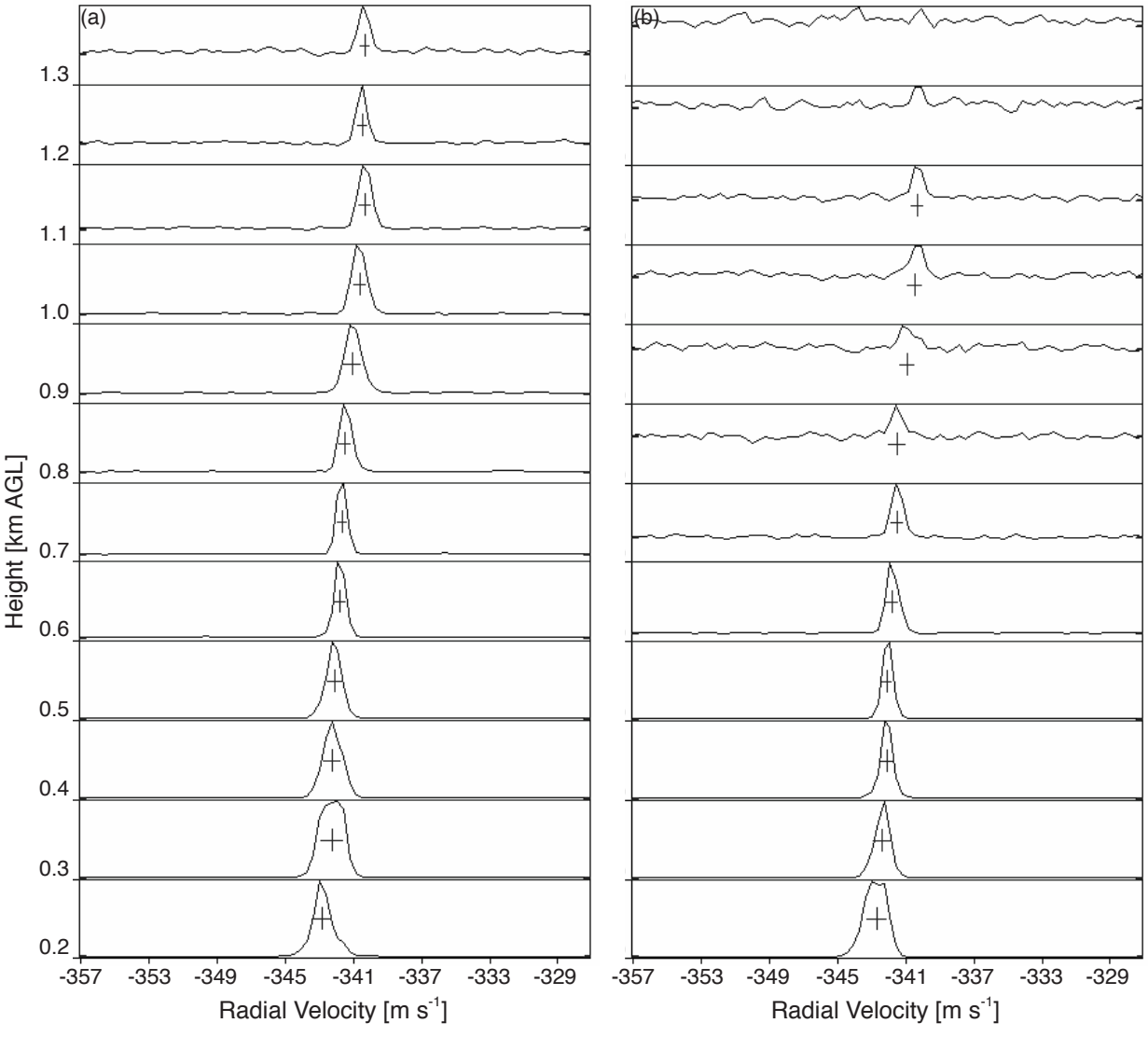

Figure 4. Doppler spectra from RASS observations measured with (a) acoustic speakers from 08:30 JST for 1 min and (b) the parametric speaker from 08:31 JST for 1 min on 19 October 2016. At each height, the first moment of the spectrum, indicated by the vertical bar, gives the vertical sound velocity, and the second moment, indicated by the horizontal bar, gives the spectral width.

Atmos. Meas. Tech. Discuss., https://doi.org/10.5194/amt-2019-92
Manuscript under review for journal Atmos. Meas. Tech.
Discussion started: 10 May 2019

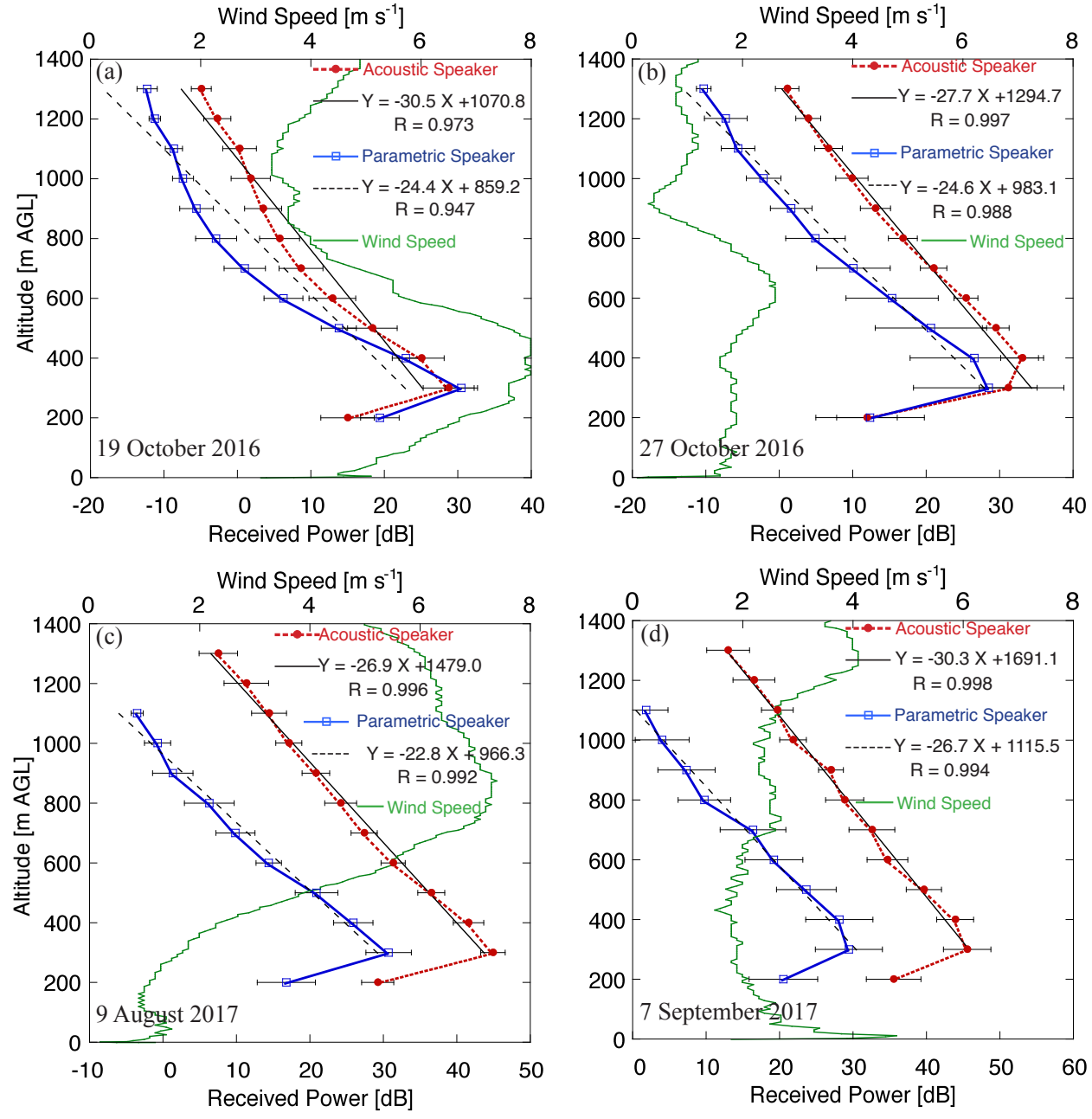

Figure 5. Profiles of received mean RASS echo power and wind speed on (a) 19 October 2016, (b) 27 October 2016, (c) 9 August 2017, and (d) 7 September 2017, derived with the acoustic speakers (red), the parametric speaker (blue), and radiosonde (green). The error bars represent 2σ. The black lines indicate linear regressions for the received power data except for the first range as shown in the upper-right legend with correlation coefficients.

Atmos. Meas. Tech. Discuss., https://doi.org/10.5194/amt-2019-92
Manuscript under review for journal Atmos. Meas. Tech.
Discussion started: 10 May 2019

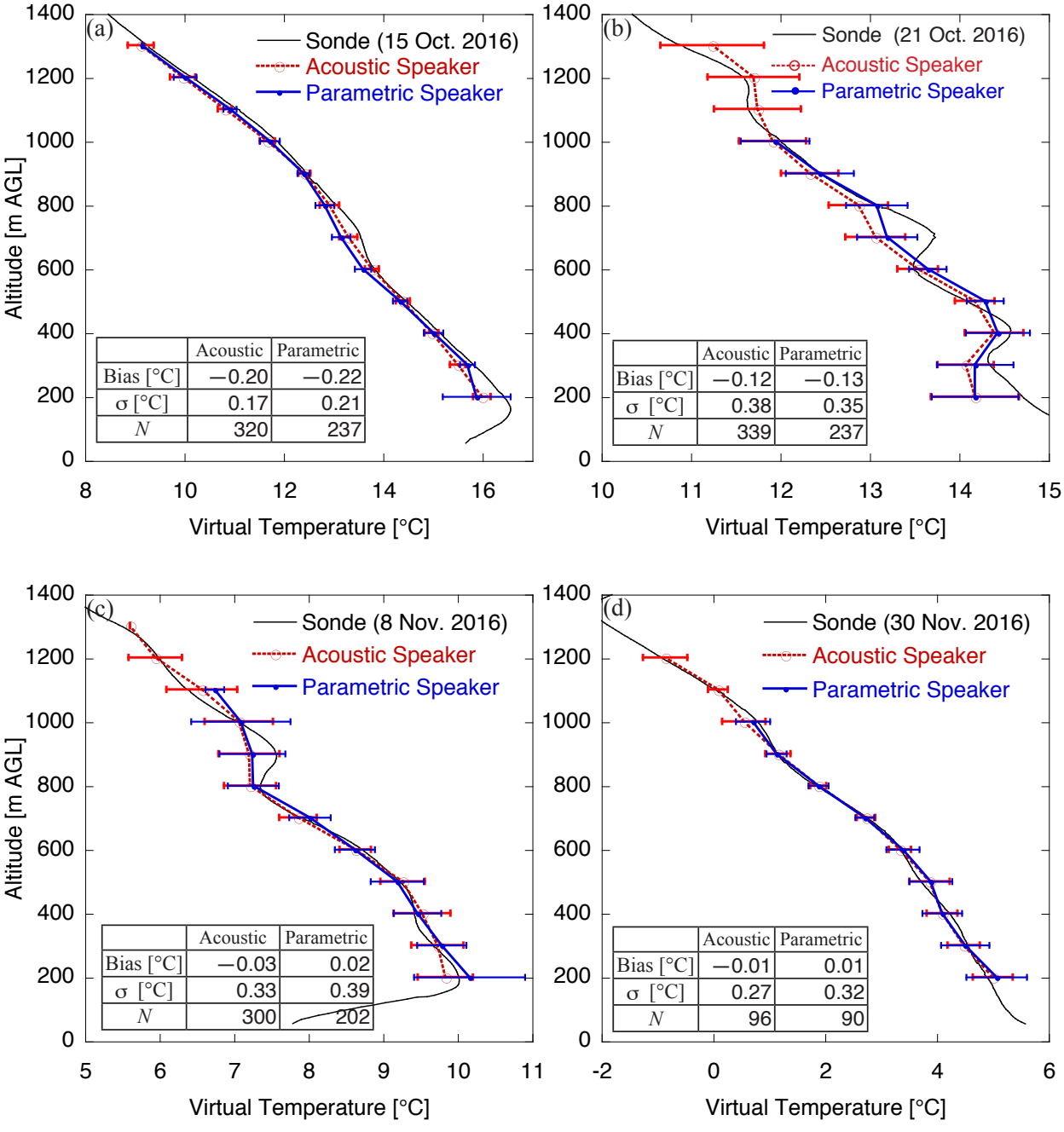

Figure 6. Profiles of virtual temperature (*Tv*) from 08:30 JST on (a) 15 October, (b) 21 October, (c) 8 November, and (d) 30 November 2016 derived from a radiosonde (black), RASS with acoustic speakers (red), and the parametric speaker (blue). The radiosonde data were smoothed by 100 m running means to match with the vertical resolution of the RASS. The error bars represent 2σ in the RASS observations. The mean, standard deviation, and number of samples of temperature difference are summarized in a table in each panel.

Atmos. Meas. Tech. Discuss., https://doi.org/10.5194/amt-2019-92
Manuscript under review for journal Atmos. Meas. Tech.
Discussion started: 10 May 2019

Atmospheric Measurement Techniques Discussions

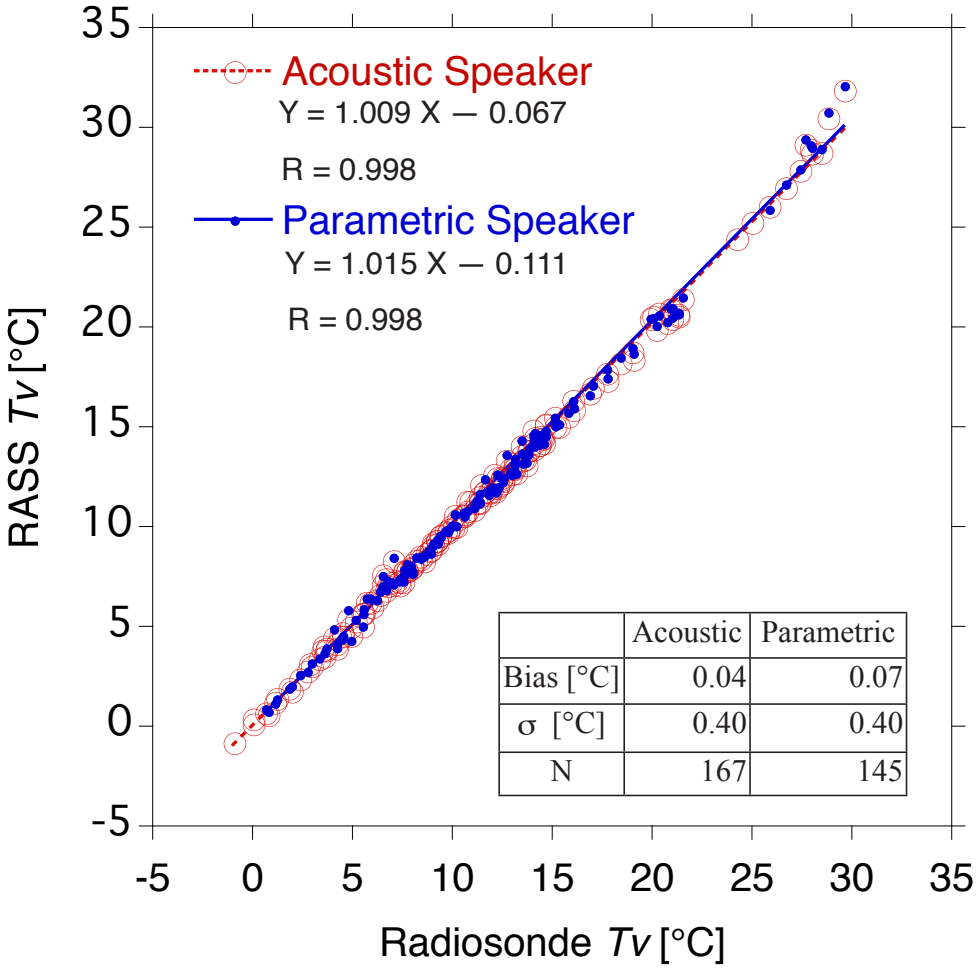

	Acoustic	Parametric
Bias [°C]	0.04	0.07
σ [°C]	0.40	0.40
N	167	145

Figure 7. Scatterplots of virtual temperature of the radiosonde vs. the RASS measurements at all heights except for the first range. The data derived from the RASS with the acoustic speakers (the parametric speaker) are plotted as open (closed) circles. The lines represent linear regressions for each data set as shown in an upper legend along with the correlation coefficients. The mean, standard deviation and number of samples of temperature difference are summarized in a bottom table.

Atmos. Meas. Tech. Discuss., https://doi.org/10.5194/amt-2019-92
Manuscript under review for journal Atmos. Meas. Tech.
Discussion started: 10 May 2019

Atmospheric Measurement Techniques Discussions

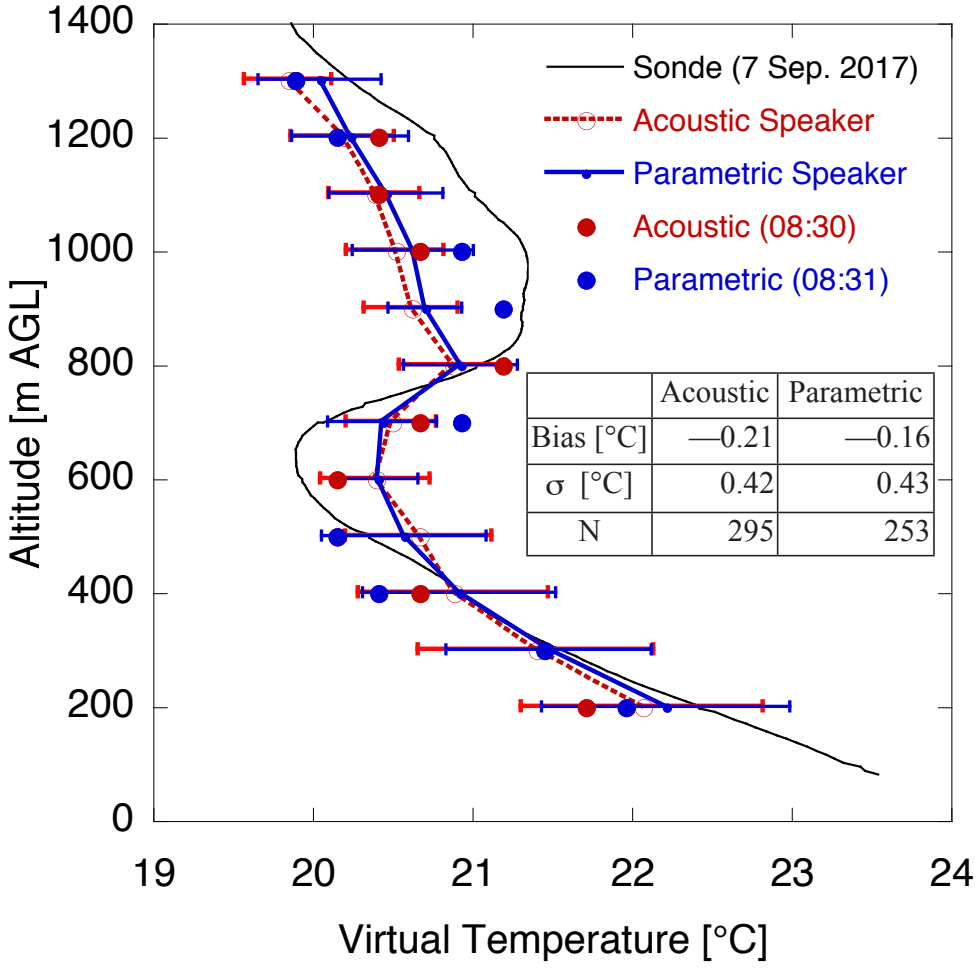

Figure 8. Profiles of virtual temperature (*Tv*) from 08:30 JST on 7 September 2017, derived from a radiosonde (black), RASS with acoustic speakers (red), and with the parameter speaker (blue). The radiosonde data were smoothed by 100 m running means to match with the vertical resolution of RASS. The error bars represent 2σ in the RASS observations averaged over 60 min, and closed circles represent 1 min raw data. The mean, standard deviation, and number of samples of temperature difference of RASS from radiosonde are summarized in the table.

Atmos. Meas. Tech. Discuss., https://doi.org/10.5194/amt-2019-92
Manuscript under review for journal Atmos. Meas. Tech.
Discussion started: 10 May 2019

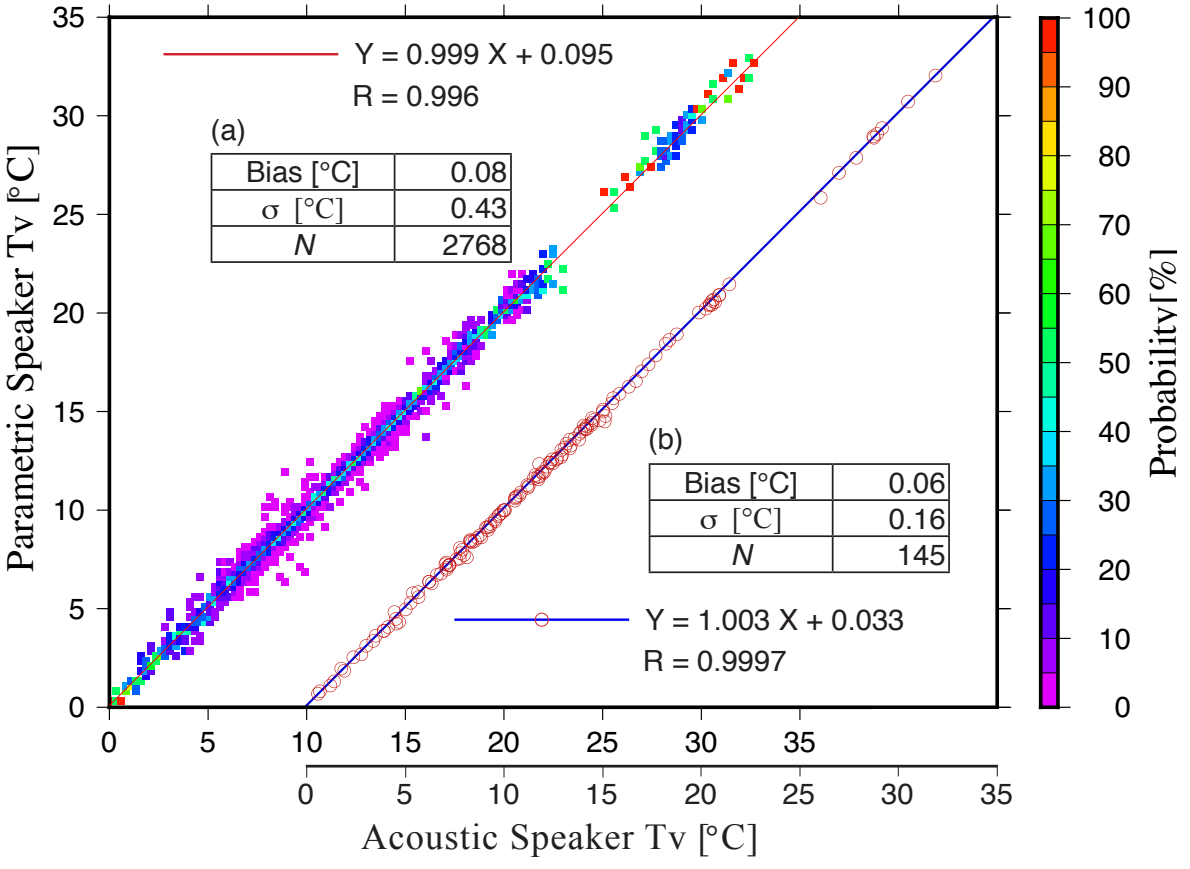

Figure 9. Comparisons of the acoustic speakers vs. the parametric speaker in measuring virtual temperature at all heights except for the first gate shown by (a) a normalized frequency diagram and (b) a scatterplot. The data obtained from each speaker system every 1 min alternately were used in (a), whereas the mean data were plotted in (b). The mean Tv derived with the acoustic speakers is shifted 10°C for ease of viewing in (b). The lines represent linear regressions for each data set, shown in the upper-left and lower-right legends along with correlation coefficients, respectively. The mean, standard deviation, and number of samples of temperature difference are summarized in each table.

Atmos. Meas. Tech. Discuss., https://doi.org/10.5194/amt-2019-92
Manuscript under review for journal Atmos. Meas. Tech.
Discussion started: 10 May 2019

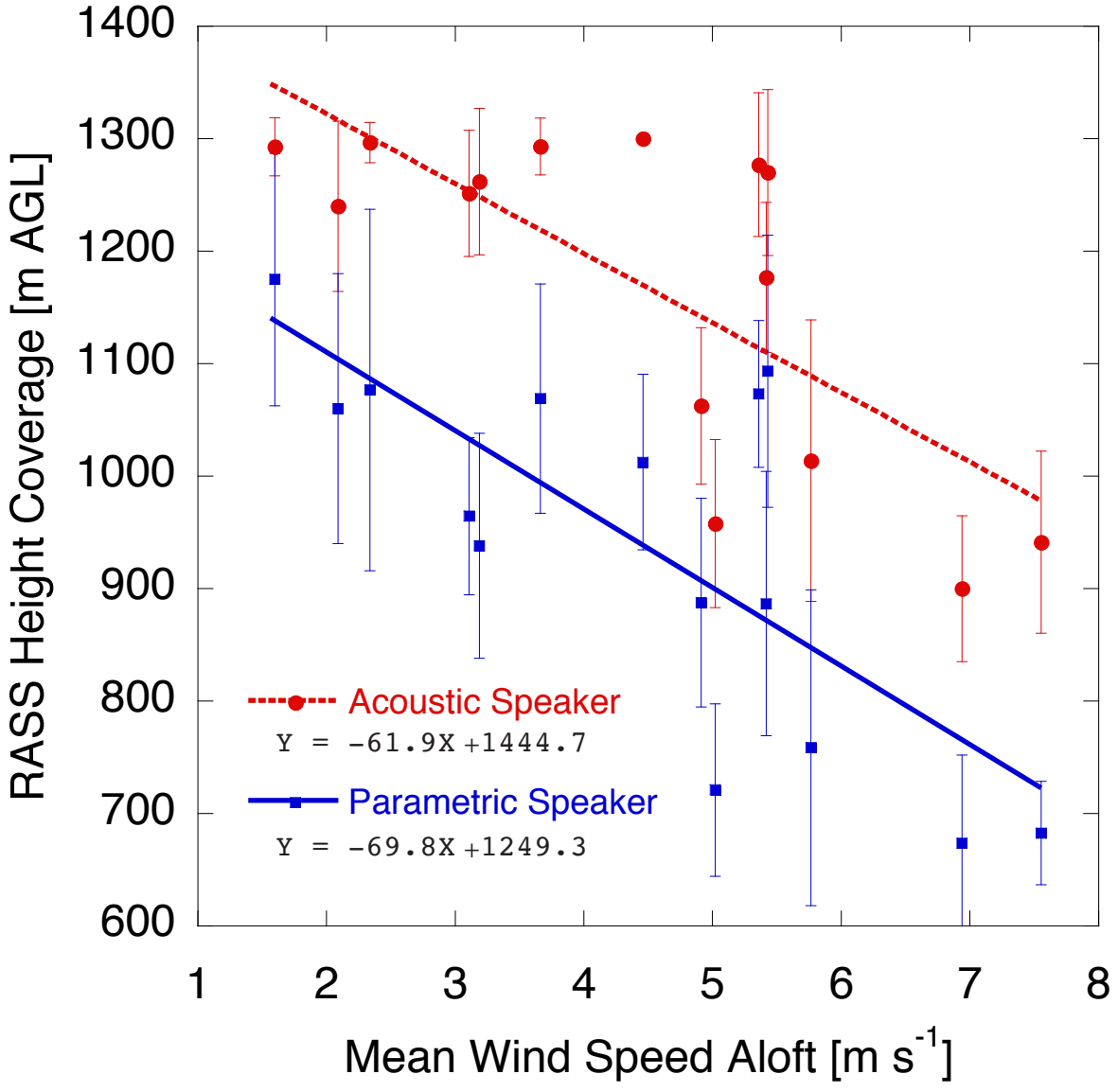

Figure 10. Scatterplots of mean height coverage of RASS measurement vs. mean wind speed aloft derived from radiosonde observations. The highest range gate sampled for the RASS measurement is 1300 m AGL. Closed circles (squares) denote observed mean RASS height coverage by acoustic speakers (parametric speaker) with standard deviations indicated by error bars. Thick lines represent linear regressions for each data set, as shown in the bottom legend.

Atmos. Meas. Tech. Discuss., https://doi.org/10.5194/amt-2019-92
Manuscript under review for journal Atmos. Meas. Tech.
Discussion started: 10 May 2019

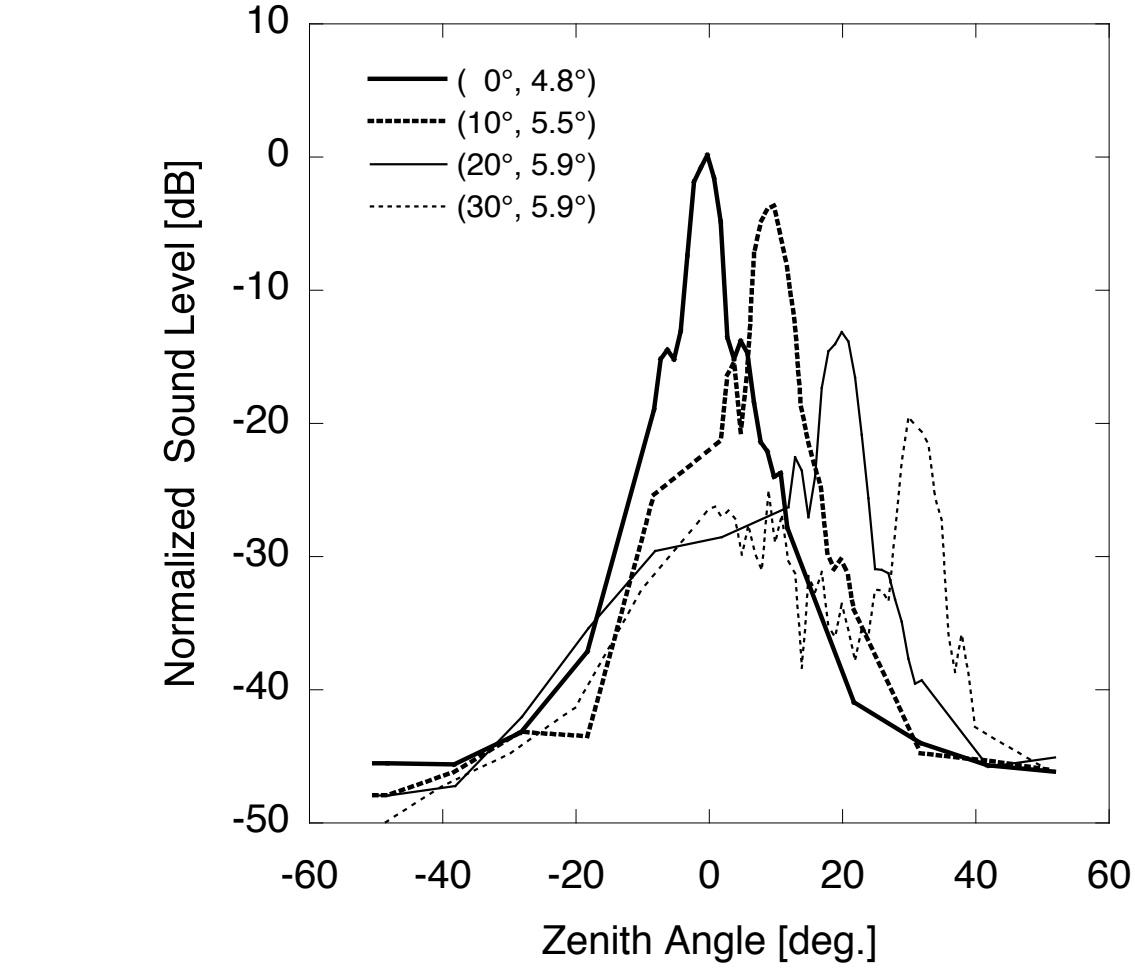

Figure 11. Normalized audible sound pressure pattern of the parametric speaker at a frequency of 3 kHz measured at multiple zenith angles, shown in the upper legend with the beam width observed. The SPL was measured with a sound level meter (Rion NL-42).